Proposal for a Forward π^0 Detector at STAR

H. M. Spinka, D. G. Underwood,
Argonne National Laboratory
Argonne, IL U. S. A.

L. C. Bland, B. Surrow, T. Ullrich,
Brookaven National Laboratory
Upton, NY U. S. A.

G. Rakness,
Indiana University Cyclotron Facility
Bloomington, IN U. S. A.

A.M. Davidenko, A.A. Derevshchikov, V.Y. Khodyrev, V.I. Kravtsov,
Y.A. Matulenko, A.P. Meschanin, V.V. Mochalov, D.A. Morozov,
L.V. Nogach, S.B. Nurushev, K.E. Shestermanov, A.N. Vasiliev,
Institute of High Energy Physics
Protvino, Russia

H. J. Crawford, J. Engelage, E. Judd,
U.C. Berkeley
Berkeley, CA U. S. A.

P. Jacobs, F. Meissner
Lawrence Berkeley National Laboratory
Berkeley, CA U. S. A.

S. Heppelmann, A. Ogawa,
Penn State University, University Park, PA U. S. A.

C. A. Gagliardi, R. E. Tribble, M. A. Vasiliev,
Texas A & M University
College Station, TX U. S. A.

G. Igo, J. Kiryluk and C. A. Whitten Jr.
UCLA
Los Angeles, CA U. S. A.

June 17, 2002

Abstract

We propose to install a Forward π^0 Detector (FPD) in STAR. Data that was obtained during the FY2002 RHIC polarized proton run demonstrates the feasibility of identifying neutral pions up to energies of about 60 GeV at large rapidity ($3 < \eta < 4$). Supplementing the capabilities of the STAR detector to identify particles at large rapidity and moderate transverse momentum allows for quantitative measurements related to several interesting phenomena. In d-Au collisions, we will measure the ratio of energetic π^0's produced in the incident deuteron direction to the corresponding yield in the direction of the incident gold ion beam. That ratio is sensitive to the gluon density in a heavy nucleus. In polarized proton-proton collisions, the analyzing power for the $p\uparrow + p \rightarrow \pi^0 + X$ reaction will be mapped out over a broad range of Feynman x and transverse momentum. In the long term, the FPD can serve as an *in-situ* polarimeter for the STAR detector, to allow the tuning of spin rotator magnets that nominally precess vertically polarized beam to provide longitudinal polarization at the interaction point. Four Pb-glass electromagnetic calorimeter modules with scintillator strip shower maximum detectors will be installed east and west of the magnet at symmetric positions left and right of the beam, on existing platforms. Four simpler calorimeters will be installed at symmetric positions above and below the beam on the east and west sides of the magnet. The electronics included will allow for the complete integration of the FPD into the STAR trigger.

Contents

1 Introduction

A prototype Forward π^0 Detector (FPD) was installed in the STAR wide angle hall, integrated with the trigger and data-acquisition systems, and operated with all of the other STAR detector subsystems during the FY2002 polarized proton run. Results from the prototype FPD demonstrate that neutral pions from ion collisions can be cleanly identified over the energy range $20 < E_\pi < 60$ GeV and at large pseudo-rapidity ($3 < \eta < 4$). With confidence gained from this experience, we propose to assemble and install a Forward π^0 Detector FPD to be used in future STAR experiments.

Forward π^0 detection capability, combined with other STAR detector subsystems that focus on mid-rapidity particle detection, provides a powerful means of attacking important problems in QCD. They include

1. transverse spin dynamics in high energy $p\uparrow + p \rightarrow \pi^0 + X$ interactions at large Feynman x,
2. small x gluon distributions, including saturation effects in heavy nuclei.

These topics address core issues that have been identified as important for the Relativistic Heavy Ion Collider (RHIC) program.

Construction of a left-right and up-down symmetric FPD will enable both short term measurements, and future applications as an *in-situ* polarimeter for the STAR spin physics program. The objective for the d-Au measurement is to place calorimeters at large $|\eta|$ on both the east and west sides of STAR (symmetric $+\eta$ and $-\eta$ coverage). This will allow a relatively unbiased measurement of the ratio of high-energy π^0 cross sections in the deuteron and gold beam directions. As discussed in more detail below, a measurement of this ratio will provide sensitivity to a possible modification of the gluon structure function for nucleons bound in heavy nuclei. The symmetry of the detector placement minimizes sensitivity to systematic errors associated with luminosity monitoring that arise when comparing yields from different collider runs.

The left-right azimuthal symmetry of the FPD is important for measuring spin asymmetries induced by collisions of vertically polarized protons. Such measurements may provide insight into the proton's transversity structure function, a leading twist distribution function that cannot be directly accessed in inclusive deep inelastic scattering because of helicity conservation. Intercomparison of transverse asymmetries with the helicity asymmetries can provide important insight into the partonic substructure of the proton. Measurements at RHIC with vertically polarized colliding proton beams can provide a timely complement to experiments aimed at understanding transversity that are currently under way around the world.

The up-down and left-right symmetry of the FPD satisfies the requirement for an *in situ* polarimeter to tune the STAR spin rotators. The rotators nominally precess vertically polarized protons to

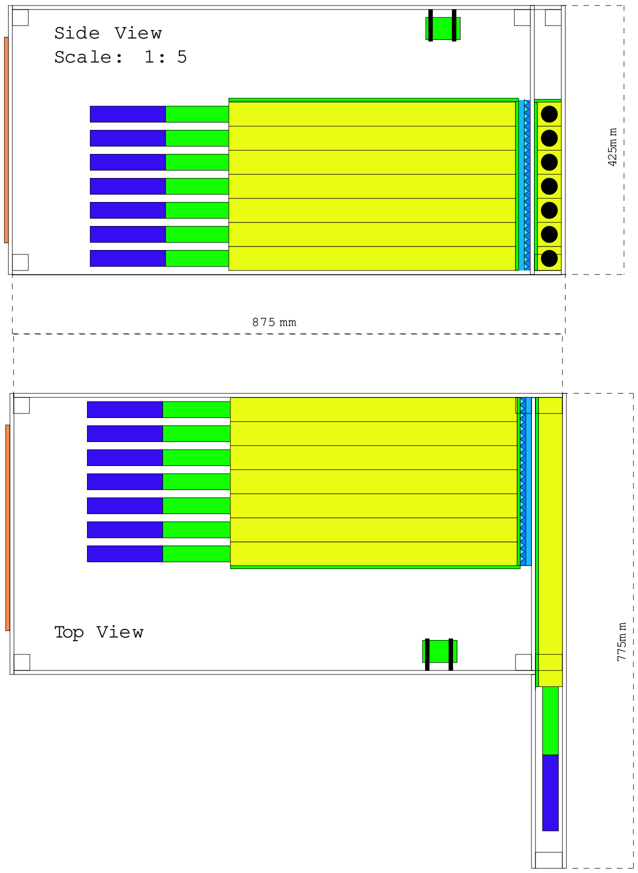

Figure 1: *Schematic of a calorimeter module proposed for the upgrade of the STAR Forward* π^0 *Detector. The module consists of a main calorimeter built from an existing 7×7 matrix of Pb-glass detectors; two 48-strip scintillator shower maximum detectors; and a 7-element Pb-glass preshower detector. A simple lead radiator must be mounted upstream of the preshower detector to optimize the efficiency of the calorimeters as a* π^0 *detector.*

produce longitudinally polarized protons at the STAR interaction region. The stable spin direction during normal RHIC operations is vertical. The spin rotators must be tuned to minimize vertical and radial polarization components. The most pernicious asymmetry that can arise from remnant vertical or radial polarization states of the two beams is A_Σ, for which there are no firm predictions from perturbative QCD and no predictable experimental signature. A non-zero analyzing power for some reaction with a large cross section can provide a high rate signal that can be used to tune the spin rotators so that there are no measured up/down or left/right spin-dependent asymmetries that can be produced, respectively, from radial or vertical polarization components of the beam.

The only reaction predicted to have a large analyzing power at RHIC energies is inclusive pion production at large Feynman x and moderate p_T. Large values for these asymmetries were measured by the Fermilab E704 collaboration at a pp collision energy of $\sqrt{s} = 20$ GeV. The analysis of STAR measurements of these asymmetries from the first RHIC polarized proton run at $\sqrt{s} = 200$ GeV is currently underway. Although the spin effects are greater for charged pion production, they require discrimination between π^+ and π^- since $A_N(\pi^+) \approx -A_N(\pi^-)$. Such discrimination in the forward direction is difficult for STAR. The predicted spin effects for neutral pion production, combined with the rate expected from the measured yield and the projected luminosity for next year's run, makes this a natural choice for polarimetry to tune the STAR spin rotators.

With these motivations, we propose to construct four electromagnetic calorimeters similar to what is shown in Fig. 1, with each calorimeter comprised of

- a 7×7 matrix of lead-glass counters with photomultiplier tubes (PMT) and voltage divider bases, built by the IHEP, Protvino group for the E-704 experiment at FNAL.
- two 48-element scintillator-strip shower maximum detectors (SMD).
- a 7-element lead-glass preshower detector. A lead radiator must be mounted immediately upstream of this preshower detector to optimize the response of the shower maximum detector.
- all calorimeters on one side of STAR would be readout using 148 channels of fast analog-to-digital converter (CDB) and FPGA (DSM) to encode the calorimeter current pulses for each bunch crossing and integrate the data from the FPD calorimeters into the STAR level-0 trigger system.
- 206 channels of an analog storage system (switched capacitor array) that can store the charge from the SMD multi-anode PMT's and the Pb-glass detector preshower detectors for each bunch crossing, and then encode the charge for a triggered event.

A schematic of the proposed calorimeters that would be mounted to the left and right of the beams on both the east and west sides of STAR is shown in Fig. 1. These proposed calorimeters

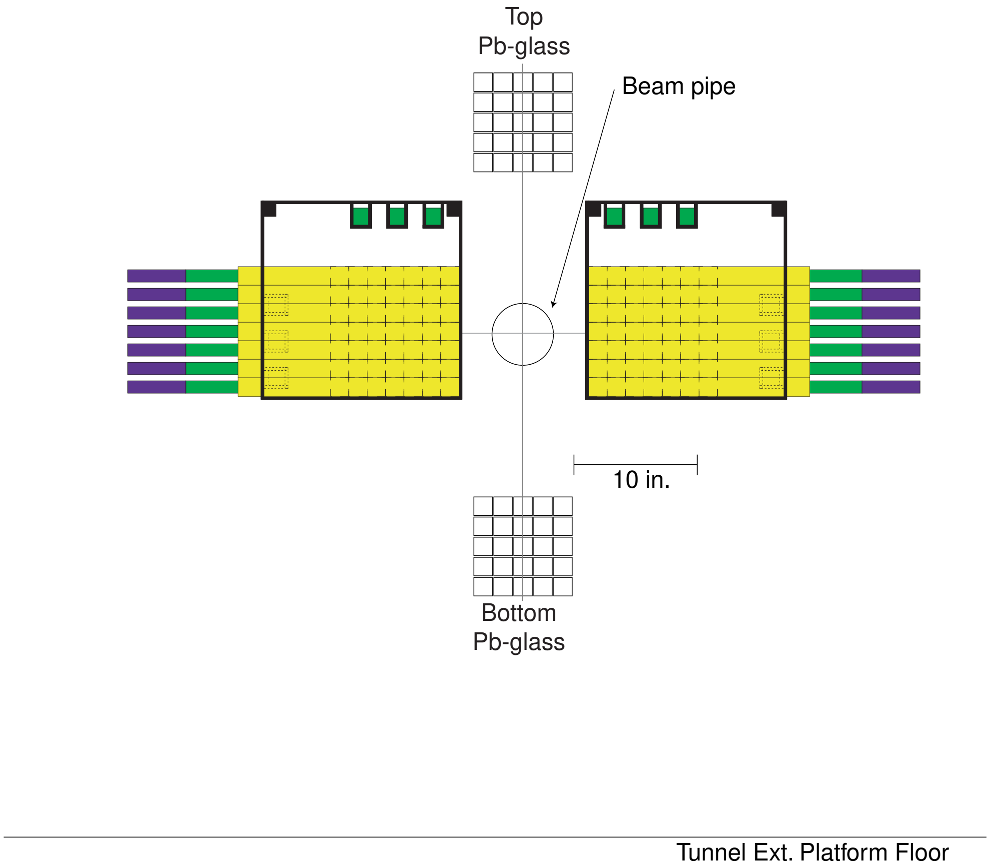

Figure 2: *Front view schematic of the deployment of calorimeters on the tunnel platform extensions on both the east and west sides of the STAR magnet. The detectors mounted to the left and right of the beam will enable complete reconstruction of neutral pions. The* 5×5 *matrices of Pb-glass detectors mounted above and below the beam serve as* in situ *polarimeters to measure radial polarization components.*

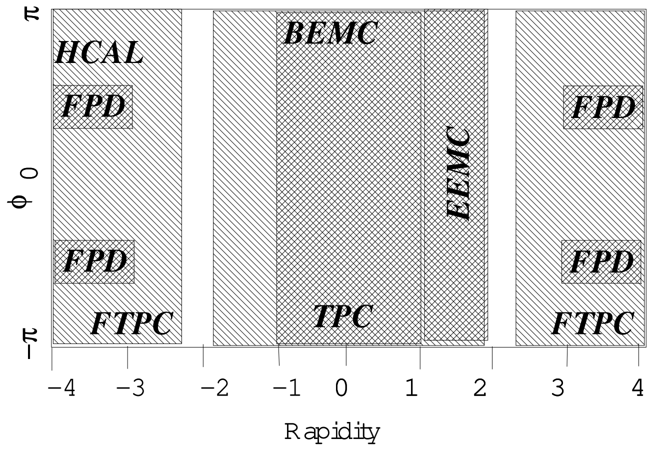

Figure 3: *Schematic showing the* η,ϕ *extent of STAR subsystems.*

play a dual role, enabling physics measurements of fast forward pions in both d-Au and $\vec{p}-\vec{p}$ collisions and serving as polarimeters to measure vertical polarization components at the STAR interaction region. In addition to these more highly instrumented calorimeters, simpler calorimeters are proposed for mounting above and below the beam pipe to serve as a polarimeter to measure radial polarization components, when spin rotators precess the vertical polarization of the proton beam to create nominally longitudinal polarization at the STAR interaction point. Each of these calorimeters consist of a 5×5 matrix of Pb-glass detectors. These calorimeters would be mounted on the east and west tunnel platform extensions in the STAR wide angle hall, approximately 750 cm from the STAR interaction point. The calorimeters would be symmetrically placed to the left and right of the beam pipe on each platform, and would provide symmetric coverage at $+\eta$ and $-\eta$. A front view of the calorimeter deployment on one side of the STAR magnet is shown in Fig. 2. The addition of the FPD would extend the capability of the STAR detector to identify particles in the large rapidity regime. A schematic of the coverage of the FPD calorimeters in η,ϕ space is shown in Fig. 3.

2 Physics Goals and Proposed Measurements

We envision three applications of the Forward π^0 Detector at STAR involving the detection of large rapidity π^0, and possibly single γ's:

- measurement of the ratio of identified particle energy spectra at $+\eta$ and $-\eta$ in d+Au collisions will provide a probe of the gluon density for nucleons bound in a heavy nucleus. Simultaneous measurements in both the direction of the deuteron and Au ion beam directions provides self calibrating sensitivities to the gluon distribution in the deuteron and Au nuclei, eliminating the need for an accurate determination of the absolute luminosity.

- in polarized proton collisions, with one proton polarized vertically, the analyzing power (A_N) for the production of π^0 mesons at large Feynman x and moderate p_T can be studied. This was the original goal for the first polarized proton run at RHIC. Analysis of data obtained from that run is currently underway. The implementation of the full FPD will enable a much more comprehensive study of spin asymmetries in the forward region during the next polarized proton run.

- In addition to tackling these interesting physics problems, a complete FPD can serve the long-term role as an *in situ* polarimeter. The need exists, because spin rotators are required to produce longitudinal polarization at the STAR interaction point, and then precess the spin back to the vertical, corresponding to the stable polarization direction of the RHIC rings.

In the following sections, each of these topics are explored in further detail.

2.1 Gluon Densities in Heavy Nuclei

The primary rationale for RHIC is to discover the Quark-Gluon Plasma (QGP), and then study its properties. To accomplish this, heavy nuclei are accelerated to high energy and then made to collide, producing final states with thousands of particles. At the partonic level, the collision can be viewed as a very large number of near simultaneous quark and gluon collisions, with the recoiling partons interacting through the extended color fields, rescattering and then fragmenting into predominantly hadrons that are observed in the final state. To reliably interpret data from relativistic heavy ion collisions it is critical to know the initial state gluon density in the colliding heavy ions.

Recent models suggest that the color fields of the colliding heavy ions are so dense as to reach saturation [1]. This is an appealing picture because of the apparent synthesis of understanding of diverse experimental results including low-x structure function measurements at HERA [2] and particle multiplicity distributions for relativistic heavy-ion collisions at RHIC. Further experimental probes of this picture are essential, and d-Au collisions at RHIC may provide a key test of the gluon saturation model [3]. Measurements with an upgraded FPD for STAR should provide the first experimental measurement of the magnitude of the gluon density in a heavy nucleus by studying neutral pion production at large rapidity in $p(d)$-Au collisions.

We know from deep inelastic lepton scattering experiments from nuclear targets, first studied at CERN, and subsequently studied at Fermilab and SLAC, that the parton distributions for nucleons in heavy nuclei are modified compared to those same distributions for free protons [4]. Deep inelastic scattering (DIS) of either muons or electrons probes partonic substructure via the exchange of virtual photons. This electromagnetic interaction provides *direct* sensitivity to the electrically charged quarks, and, at best, only *indirect* sensitivity, through scaling violations [5], to the electrically neutral gluons. Analyses of the A dependence of DIS over the limited Q^2 range covered by existing measurements suggests that shadowing effects will also be present for the gluons confined within nucleons that are bound in heavy nuclei [6]. The study of p+Au (or, d+Au) collisions at RHIC will provide the first opportunity to *directly* probe gluon densities in heavy nuclei, by using quarks to directly couple to the gluon's color charge.

A nearly unique way to probe gluon densities is via the detection of direct photons, produced in hard scattering collisions via the quark-gluon Compton process. In pp collisions, backgrounds from $q\overline{q}$ annihilation into $\gamma + g$ final states are small because the gluon density is larger than the antiquark density. Experimentally, it is very difficult to access direct photons at high energies because of the diphoton background arising from the decay of neutral mesons and from single photons that result from the fragmentation of final-state quarks and gluons. Single photon detection may be possible with an upgraded FPD, but is not the primary focus of this proposal.

Initial sensitivity to gluon densities in Au nuclei can be obtained from the study of qg elastic scattering. In general, jets are produced in pp collisions via a multitude of partonic subprocesses, involving gg, qg, $q\overline{q}$ and qq' initial states. The admixture of different partonic initial states is maximal when hadronic jets are observed at midrapidity. Particle detection in the forward, large rapidity, direction reduces this initial-state ambiguity using simple kinematics. When collinear partons collide, the final state products are characterized by three quantities:

- a transverse momentum p_T, related to the fraction, x_T of the kinematic maximum transverse momentum via $x_T = 2p_t/\sqrt{s}$
- the scattering angle (θ_1) of one of the final state products, most frequently expressed as a pseudorapidity ($\eta_1 = -\ln[\tan\theta_1/2]$).
- the scattering angle (θ_2), or the pseudorapidity η_2, of the other final state product.

For a $2 \to 2$ process involving collinear initial state partons, there are simple interrelationships between the momentum fractions or Bjorken x values for the colliding partons, x_1 and x_2, in the initial state and the final state kinematic quantities:

$$x_{\pm} = \frac{x_T}{2}(e^{\pm\eta_1} + e^{\pm\eta_2}) \tag{1}$$

When one of the final state particles is detected at large pseudorapidity, these kinematic relations simplify to $x_+ \approx \frac{x_T}{2}e^{\eta_1}$ and $x_- \approx \frac{x_T}{2}e^{-\eta_2}$. For positive η_2, x_- is small and approaches zero when both final state particles are detected at large pseudorapidity. So as not to exceed the kinematic limit, $\eta_1 < \ln(2x_1/x_T) \approx \ln(1/x_T)$, choosing a valence-like value for x_1 of 0.5. For p_T=2 GeV/c, x_T=0.02, and $x_+ = 0.5$ is achieved with $\eta_1 = 3.9$. A large enough value of p_T is required to interpret large rapidity particle production as arising from $2 \rightarrow 2$ interactions involving the partons within the proton. At collider energies, recent next-to-leading-order perturbative QCD calculations [10] successfully describe mid-rapidity charged hadron cross sections down to $p_T \sim 2$ GeV/c. The bottom line is that forward detection of final state products emphasizes collisions where a large x parton, traveling in the direction of the detected forward particle, collides with a small x parton from the other nucleon. Large x partons are most probably valence quarks, and small x partons are most probably gluons.

These simple ideas are supported by PYTHIA [11] simulations of high energy π^0 production ($E \geq 20$ GeV) at large pseudorapidity ($3 \leq \eta \leq 4$) in pp collisions. The dominant subprocess that leads to the π^0 production is found to be qg elastic scattering. The Bjorken x range of the gluon varies in the interval $10^{-3} \leq x_{gluon} \leq 10^{-2}$, with the smallest value being the most probable. Essentially, forward π^0 production is analogous to a partonic fixed target experiment, where an energetic quark from one proton scatters from a very low momentum gluon from the other proton.

The basic idea of positioning calorimetry symmetrically at $+\eta$ and $-\eta$ for a d+Au collision run is to form the ratio of the detected particle energy distributions, measured simultaneously at the two ends of STAR thereby eliminating the need to carefully measure the absolute collision luminosity. The cross section ratio is given by

$$\frac{d^2N/dEd\eta|_{+\eta}}{d^2N/dEd\eta|_{-\eta}} \sim \frac{q_d(x_1) \bigotimes g_{\mathrm{Au}}(x_2) \bigotimes \hat{\sigma} \bigotimes D(z)}{q_{\mathrm{Au}}(x_1) \bigotimes g_d(x_2) \bigotimes \hat{\sigma} \bigotimes D(z)}, \tag{2}$$

representing the ratio of the convolutions of the quark density, $q(x_1)$, in the deuteron (Au ion), the gluon density, $g(x_2)$, in the Au ion (deuteron), a partonic hard scattering cross section, $\hat{\sigma}$ and a fragmentation function, $D(z)$. The cross section ratio provides sensitivity to the gluon density in the Au nucleus.

Further insight regarding the gluons in Au can be obtained by studying the dependence of the forward π^0 cross section ratio on the charged particle multiplicity measured at rapidities close to the Au beam. Such measurements can be concurrently made at STAR by counting charged particle tracks in the Forward Time Projection Chamber (FTPC) ($2.5 \leq \eta \leq 4$) or by measuring energy loss in the Beam-Beam Counter ($2.5 \leq \eta \leq 5$). The charged particle multiplicity will provide some measure of the centrality of the interaction that leads to forward π^0 production.

Recently, the possibility of probing the gluon density in heavy nuclei via pion production at large rapidity in d-Au collisions has been recognized by others [3]. In their picture, specific $2 \to 2$ scatterings are not identified, rather the notion is to use quarks from the proton to probe the gluon field of a heavy nucleus. The prediction is that the jet cross section is modified from the simple pQCD expectation of $1/p_T^4$ to a much less pronounced falloff at high energies of $1/p_T^2$ if there is gluon saturation in heavy nuclei. To date, there are not numerical predictions of the expected p_T dependence of observable particles such as π^0's, but the authors argue that detecting mesons at large rapidities provides a robust manner to test the gluon saturation model.

All of these simple arguments ignore important effects such as intrinsic transverse momentum (k_T) of the partons, and initial and final state hadronic or partonic interactions, leading to energy loss and multiple scattering. These effects can alter the yield, and its p_T depedence, when comparing π^0's produced in the direction of the deuteron beam to those produced in the direction of the Au beam. In their own right, it is important to gain a quantitative understanding of these effects to accurately model the dynamics of relativistic heavy ion collisions. It is expected that first measurements of the type outlined above will provide an important stimulus to theory, and will ultimately lead to increased understanding of gluon density differences for free nucleons and heavy nuclei.

We propose to simultaneously measure in d+Au collisions at $\sqrt{s_{NN}}$ the π^0 energy distributions in the direction of both the deuteron beam and Au beam in the STAR wide angle hall at large pseudorapidities, $3 \leq |\eta| \leq 4$. FPD calorimeter modules mounted on the east and west tunnel platform extensions, as described in Sec. 4, will enable these measurements.

2.2 Transverse single spin asymmetries

When a transversely polarized proton collides with another proton most of the energy from the polarized proton may emerge from the interaction as an energetic pion. When this happens, E704 discovered [14, 15] in fixed target experiments at Fermi Lab with beam polarized in the vertical direction, that positive pions mostly go to the left and the negative pions mostly go to the right. This effect is not subtle but characterizes the typical behavior, with up to 3/4 of the pions on a particular side (left/right) following the pattern. Neutral pions, to a slightly lesser degree follow the positive pions. This remarkable pattern occurs at a transverse momentum of order 1 GeV/c which by the uncertainty principle represents scattering from a coherent region much smaller than the size of the 1 Fermi proton.

Common sense suggests that this remarkable result should reflect the scattering of constituents within the nucleon. The natural interpretation is that these events are associated with initial state fluctuations in which a single quark in the nucleon carries most of the proton momentum. The

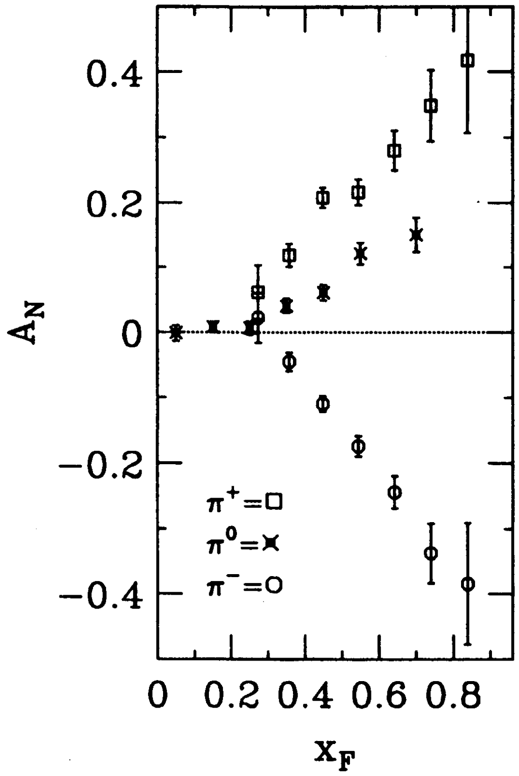

Figure 4: *Results from FNAL experiment E704, showing the analyzing power for charged [15] and neutral [14] pions produced when a 200 GeV/c tertiary polarized proton beam interacts with a stationary proton target.*

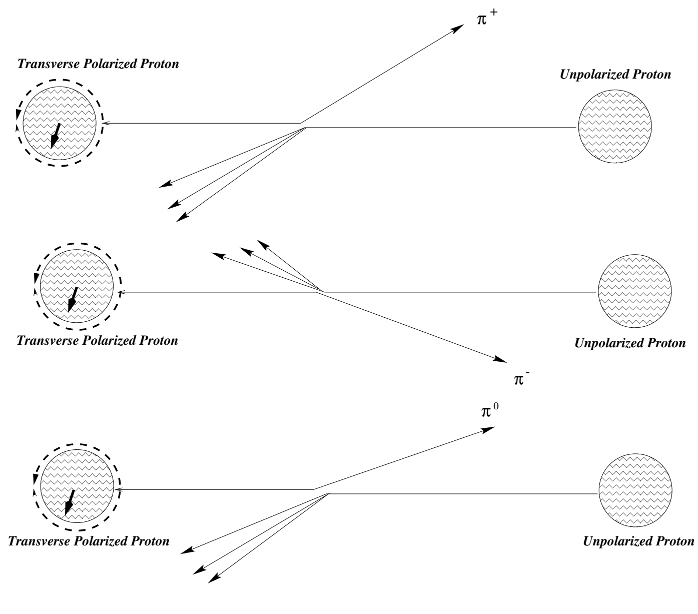

Figure 5: *For pions produced at $x_F > 0.7$ and $p_T > 0.7\ \frac{GeV}{c}$ it was observed by E704 that a transversely polarized initial proton produces pions that are isospin separated. The initial state proton spin is out of the page and positive x_F is the fragmentation region for the polarized proton.*

candidate subprocess for such scattering is the interaction of a large x (momentum fraction) up quark to make a π^+ or a large x down quark to make π^-. Because there are more large x up quarks than down quarks in a proton, leading to a larger π^+ cross section than π^- cross section, it is not too surprising that the π^0 events also come mostly from up quarks. This intuitive picture can also be consistently applied to E704 data on the interactions between protons and transversely polarized anti-protons where the signs of asymmetries of π^+ and π^- are reversed.

In contrast to this intuitive interpretation, it has long been known that Perturbative QCD makes the clear prediction when an isolated transversely polarized quark scatters from another parton, the single spin asymmetry should be proportional to $\frac{m_q}{\sqrt{s}}$ with m_q the mass of the quark and $\sqrt{s}$ the energy in the center of mass of the parton pair. To many it was surprising that these asymmetries did not seem to vanish with increasing energy. However it has become clear in the last decade that it is natural for the quantum mechanical wave function of quarks in the nucleon to provide a correlation between k_t, the internal transverse momentum of the quark, and the transverse spin of the quark[16, 17]. In such a case, the single spin asymmetries need not become small at large energies but could scale as $A_n \propto \frac{k_t}{p_t}$ with p_t the transverse momentum a daughter pion from the quark fragmentation. Not only are large asymmetries allowed but if present they provide crucial information about the correlations between spin and other kinematic quantities like flavor and transverse momentum within the proton wave function. It has been argued that these observables may provide the most direct insight about the role of chiral symmetry breaking in the nucleon wave function[18]. The quark polarization distributions in both longitudinally and transversely polarized protons are basic building blocks in the characterization and understanding of the structure of the proton. The relationship between longitudinal and transverse spin structure is non-trivial. The difference in these distribution depends directly upon the QCD structure of the nucleon bound state system.

While much has been learned about the longitudinal spin structure of nucleons from electron interactions, little is known about the transverse structure. In the last decade, it has been widely acknowledged that one of the most important spin physics objectives for RHIC is to characterize the distributions of transverse polarization for the quarks in the transversely polarized proton.

Common sense tells us that the basic features of the single spin asymmetries A_n for pions observed in E704 and other experiments, directly reflect these transverse spin distributions. The challenge for PQCD has been to transform that statement into a well defined formalism. However formal methods of PQCD, as they existed 10 years ago when these data were obtained, could not make the common sense connection in an unambiguous way. Indeed, theorists were still in the process of overturning a false prejudice that the vanishing of these asymmetries at high energy was a firm prediction of QCD. But in the last few years that situation has changed very dramatically. The experts in QCD are now expressing the greatest interest in studying these effects, with models that can connect these large transverse spin effects with the essential nature of the nucleon state [19].

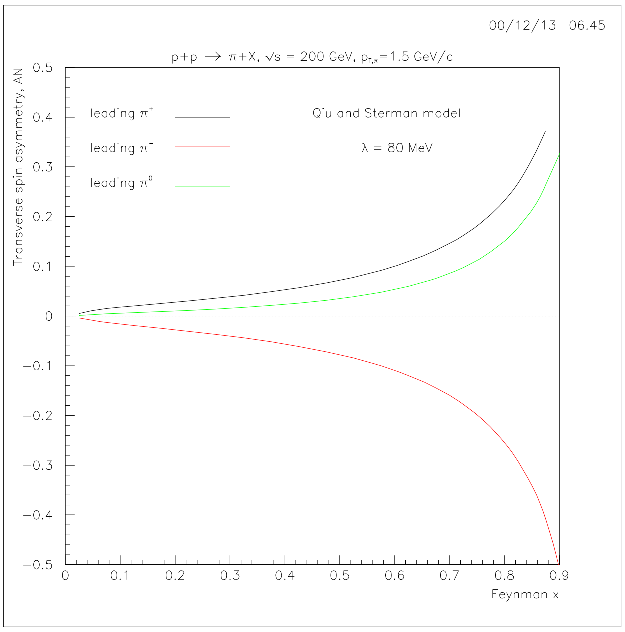

Figure 6: *Theoretical predictions for the variation of the analyzing power of large-rapidity pions produced in the collision of vertically polarized protons at* $\sqrt{s} = 200$ *GeV. This particular model [21] attributes the single spin asymmetry to a twist three effect in the hard scattering. Other models attribute the dynamical origin to either* k_T *dependent distribution or fragmentation functions, and predict similar effects for* A_N *at RHIC energies.*

There has been renewed interest in the analyzing powers observed by the E704 collaboration for the $pp \to \pi + X$ reaction, for pions produced at large Feynman x and moderate p_T. The recent interest arises from the transverse spin asymmetries observed in semi-inclusive deep inelastic scattering by the HERMES [7] collaboration. Their observation is an azimuthal angle dependence for π^+ and π^0 mesons detected in coincidence with a charged lepton that has undergone deep inelastic scattering. This spin effect has been interpreted as evidence of Collins fragmentation [8], a $k_\perp$ dependent fragmentation function that analyzes transverse quark spin, resulting in an azimuthal modulation of pions. This chiral-odd function is convoluted with a chiral-odd distribution function so that the overall chirality in the scattering is even. The distribution function claimed to be responsible for the transverse spin effects in semi-inclusive deep inelastic scattering is the transversity function, representing the difference in probability of finding a quark with its spin parallel *vs* antiparallel to a transversely polarized proton in the infinite momentum frame. Attempts are underway to perform a global analysis of the E704 analyzing powers and the azimuthal spin asymmetries observed in semi-inclusive deep inelastic scattering.

The recent interest in this wide range of transverse polarization effects has inspired an ongoing reevaluation of some of the principles underlying the factorization in hadronic interactions [20]. A framework is emerging in which the PQCD analysis of single spin pion asymmetries will be much more natural than it has been in the past. The puzzle of large values for A_N at high energies has evolved toward a natural theoretical consequence of QCD, reflecting the nature of the nucleon bound state. Many models that claim to describe the E704 spin asymmetries now also predict the persistence of these transverse single spin asymmetries for large rapidity pion production at RHIC energies (see Fig. 6).

Measurement of analyzing powers for pions produced in $\vec{p}-\vec{p}$ collisions in comparable x_F and p_T ranges at RHIC, with a minimum of $10\times$ greater collision energy than for the E704 experiment at Fermilab, can establish the dependence of A_N for pion production on center of mass energy, p_T and x_F. If a program of p-A collisions studies is embarked upon at RHIC, it would be possible to do so with polarized proton beams to study how the nuclear medium alters these spin effects. To probe a similar x_F and p_T regime as studied by the E704 collaboration at RHIC requires the addition of far forward calorimetry. The STAR endcap electromagnetic calorimeter extends to η=2. A neutral pion produced with x_F=0.5 at this pseudorapidity has a transverse momentum of $\sim$13.5 GeV/c, well beyond the p_T range of the E704 experiment. With the FPD addition, a 50 GeV π^0 detected near $\eta = 4$ has a transverse momentum of $\sim$ 2 GeV/c.

Finally, the STAR apparatus provides an ideal environment for the detailed study of this phenomena that will be necessary to distinguish between the classes of models. The wide coverage of the central Time Projection Chamber and the Forward Time Projection Chambers of the STAR detector allows us to characterize not only the distribution of π^0's but also the overall charged particle structure of the event from rapidity -4 to +4.

For example, we can ask if the asymmetry observed for the π^0 is correlated with the distribution of other charged tracks throughout that wide range of rapidity. Most interesting is the idea associated with the Collins effect, that the π^0 asymmetry reflects an asymmetry in the fragmentation of the quark jet. Such a model would require the jet axis to systematically differ from the π^0 direction. Additional jet fragments observed in the FTPC will be directly observed in STAR. A systematic azimuthal angular dependence between the π^0 direction and the direction of other jet fragments will be directly observable as a function of beam polarization. Similar correlations can be studied for fragments in other regions of rapidity as well.

It has been noted that a future addition of a simple hadronic calorimeter for triggering would enable a similar measurement of charged pion asymmetries with charged pion tracks observed in the FTPC. It may be possible, with full azimuthal jet coverage in the central rapidity region, to trigger on moderate p_T in the forward region by demanding missing p_T in the central rapidity calorimeter and tracker.

2.3 Spin Rotator Magnet Tuning

Polarized beams in the RHIC accelerator require the use of Siberian Snakes to overcome depolarizing resonances. With two Snake magnets operating in each ring, the stable spin direction for the stored proton beam is vertical. The study of gluon polarization and the study of the flavor-dependent decomposition of the nucleon's spin via $W^{\pm}$ production require longitudinal polarization for the colliding proton beams. Spin rotator magnets mounted in both rings on either side of the STAR (and PHENIX) interaction point will be installed in the summer of 2002 to precess the polarization from vertical to longitudinal and then back again. Polarimeters mounted elsewhere in the RHIC ring will measure the magnitude of the beam polarization, but cannot establish that protons collide at the STAR interaction point with purely longitudinal polarization. That determination must be made using *in situ* polarimeters, sensitive to the direction of the polarization vector of the colliding proton beams.

Most vertical or radial polarization observables result in a azimuthal (ϕ) variation of particles produced in a polarized proton collision. From much lower energy $\vec{p}-\vec{p}$ interactions [9], it is known that one such two-spin observable (A_{Σ}) depends only on the relative polarization directions of the colliding protons, and does not have an azimuthal harmonic modulation of the particle yield, correlated with the incident proton spin directions. If the polarization vector of the colliding polarized protons has significant vertical and/or radial components, then the resulting two-spin asymmetry will be a linear combination of A_{LL} and A_{Σ}. There is no theoretical guidance about the possible magnitude of A_{Σ} at RHIC energies. There have been predictions [10] for A_{TT}, a vertical two-spin asymmetry that has a $\cos 2\phi$ modulation of the particle yield. Even for maximal transversity structure functions that saturate the Soffer bound [12], the mid-rapidity A_{TT} effects are expected to be small (albeit interesting in their own right to measure) implying little utility as a means of tuning the spin rotator magnets.

We propose to use the expected non-zero analyzing power for π^0 production at large Feynman x and moderate p_T as a means of setting the spin rotator magnets to produce longitudinal polarization, and then provide a continuous monitor of their performance during runs that aim to measure longitudinal two-spin asymmetries. A robust result for this analyzing power must be obtained prior to using this process as a tool for the STAR spin program.

The accuracy that can be obtained from the FPD as a local polarimeter can be estimated from yields measured with the prototype FPD (more details can be obtained in the Appendix) and the theoretical prediction for the analyzing power for π^0 production. The analysis of spin effects obtained with the prototype FPD is still underway. For RHIC fill 2207, data recording started when the collision luminosity was 1×10^{30} cm^{-2} s^{-1}. In the fill, a total of 16 nb^{-1} was recorded by the data acquisition system (DAQ), and the average luminosity over the 6.9 hour life of the fill was a factor of two smaller than the peak luminosity. A total of 76K π^0 events were reconstructed for the fill with energies greater than 25 GeV. This number is corrected for the DAQ live time, but not for the π^0 reconstruction efficiency. From the measured variation of the yield with energy, and the predicted variation of A_N (Fig. 6), we expect an effective analyzing power of $\overline{A_N} \sim 0.02$ for π^0's produced with energies greater than 25 GeV. This effective analzing power would provide sensitivity to a vertical or radial polarization component of $\sim$10% for data acquired in a fill that delivers 160 nb^{-1} based on statistical errors alone, assuming a left/right symmetric polarimeter arrangement of the calorimeters. For larger effective analyzing powers, the sensitivity to these unwanted polarization components increases.

3 Summary of Prototype FPD Performance and Monte Carlo Simulations of FPD

3.1 Neutral Pion Decay

It is useful to review the basic kinematics of $\pi^0 \to \gamma\gamma$ decay, and how those kinematics affect high-energy π^0 detection. The decay is particularly simple to simulate, because the π^0 is a pseudoscaler meson, and hence its decay to two photons is isotropic in its rest frame. The resulting photon pairs that are produced by the high energy neutral pion are characterized by an opening angle distribution and an energy sharing distribution. The latter is defined as

$$z_\gamma = \frac{|E_{\gamma 1} - E_{\gamma 2}|}{E_{\gamma 1} + E_{\gamma 2}}, \tag{3}$$

and is a uniform distribution, varying from 0 to $1 - m_\pi c^2/E_\pi$, which is nearly unity at large pion energies. The opening angle distribution is very strongly peaked at the minimum opening angle given by

$$\sin\phi_{\gamma\gamma}^{\min} = \frac{2m_\pi c^2}{E_\pi}, \tag{4}$$

but, extends to $\phi_{\gamma\gamma} = \pi$, because the photons are massless. These two kinematic variables are interrelated: large z_γ corresponds to large $\phi_{\gamma\gamma}$. The probability that an energetic π^0 will decay with $\phi_{\gamma\gamma}$ substantially larger than $\phi_{\gamma\gamma}^{\min}$ is quite small.

In the simple simulation, monoenergetic π^0's uniformly populate narrow pseudorapidity and azimuthal angle intervals, and originate from a Gaussian distributed source, representing the collision diamond, that is displaced by 750 cm along the beam line from the detector. The detector transverse dimensions are set to correspond to the size of the north calorimeter used during the FY2002 polarized proton run. Events are distinguished into two classes: for one class both decay photons are contained within the detector transverse dimensions; for the other class only one decay photon is contained, and the other photon escapes detection. The resulting energy sharing distribution is shown in Fig. 7. The transverse dimensions of the north calorimeter used in the prototype FPD provides good acceptance over a broad range of photon energy sharing, corresponding to complete acceptance for opening angles near $\phi_{\gamma\gamma}^{\min}$. The z_γ distribution is in agreement with what was observed during the experiment. The gradual falloff at the largest z_γ arises because of the large diamond size. By reducing the diamond size, the falloff at large z_γ is much more rapid, implying complete acceptance for the daughter photons for up to 80% of the decay phase space.

As the detector size is decreased, the probability to detect asymmetric π^0 decays decreases, and the containment of both daughter photons within the calorimeter decreases. In the case where normalized yields are desired, such as for comparing π^0 spectra at $\pm\eta$ in a d-Au run, sufficient detector size is required to provide good containment of the decay photons to minimize the sensitivity to geometrical

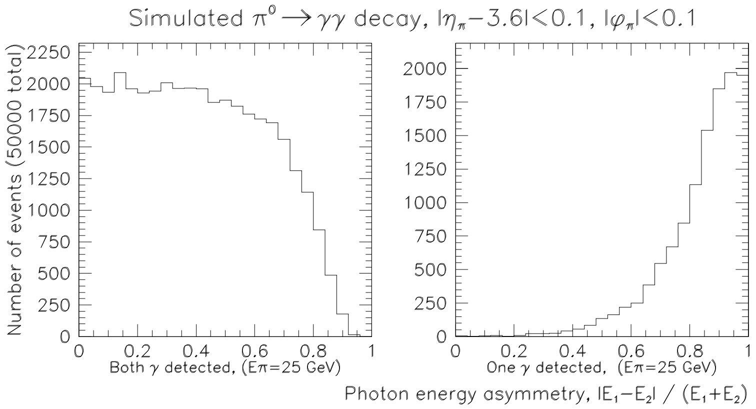

Figure 7: *The distributions result from a simple simulation of $\pi^0 \rightarrow \gamma\gamma$ decays. Each distribution corresponds to the photon energy sharing, defined in the text. For the simulation, π^0's are selected at random from a narrow pseudorapidity and azimuthal angle interval from a Gaussian distributed source located 750 cm from the detector. Events in which both decay photons are contained within the detector transverse dimensions populate the distribution at the left. Events where only one decay photon is contained populate the distribution to the right.*

errors in mounting the calorimeters. Poor containment probability also increases the background in the invariant mass spectrum. One component of that background is single photon events that are misidentified as diphoton events because of fluctuations in the single photon transverse shower profile measured by the shower maximum detector planes.

3.2 Results from the prototype FPD

As anticipated [13], invariant mass resolution is most dependent on an accurate determination of the diphoton opening angle, and is only coarsely dependent on the measurement of the individual photon energies. This is confirmed by the measurements completed with the prototype FPD that included a scintillator strip shower maximum detector to make the requisite opening angle measurement, spanning the full range of neutral pion energies that can be produced from $\sqrt{s} = 200$ GeV pp collisions (Fig. 8). For this data, the mass resolution was limited by the extent of the vertex distribution for the colliding protons. Future operation of the RHIC rings with the 200 MHz storage cavities will reduce this contribution to the mass resolution.

Other pertinent information obtained from the prototype FPD includes:

- The particle flux in the vicinity of the DX magnet in the STAR Wide Angle Hall predominantly arises from ion collisions rather than from beam-gas backgrounds. The latter contribution is observed to vary for different fills of RHIC, but can be minimized by suitable collimation.

- The detector response was uniform and stable over time. This means that virtually all of the features of the events observed are those expected from $\pi^0 \rightarrow \gamma\gamma$ decay, for neutral pions

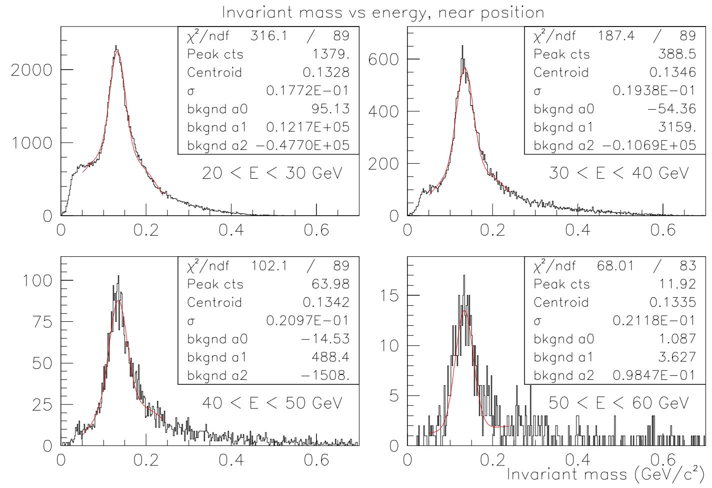

Figure 8: *Reconstructed invariant mass of events obtained from polarized proton collisions at* $\sqrt{s}$*=200 GeV with identified cluster pairs selected on the total energy in the calorimeter towers. The invariant mass resolution is robust up to 60 GeV and is expected to persist up to* π^0 *energy of 100 GeV. For higher energies, the diphoton minimum opening angle is too small to resolve using the scintillator strip shower maximum detector.*

boosted by Lorentz factors of ≥ 150.

- The energy scale of the calorimeter can be determined by an *in situ* calibration that assures that the diphoton invariant mass peak corresponds to the physical π^0 mass.

To summarize, the feasibility of identifying neutral pions at large rapidity and moderate transverse momentum was clearly established during the first RHIC polarized proton collider run at $\sqrt{s}$=200 GeV. Details of the performance of the prototype FPD are provided in the Appendix. Analysis of the spin dependence of the yields is still underway.

3.3 FPD performance simulations

The essential components of a detector that aims to identify very high energy neutral mesons is

- a calorimeter that measures the total energy of the decay products of the meson. Segmentation of the calorimeter can be used to measure the opening angle between the two photons. At the very high meson energies that will be probed by the FPD, this is not practical.
- a means to accurately determine the opening angle between the daughter photons. We propose to use scintillator strip shower maximum detector (SMD) technology for this measurement.
- a sufficiently thick radiator to initiate the electromagnetic showers of the daughter photons prior to the SMD. We propose to use a partially active radiator to serve as a preshower detector.

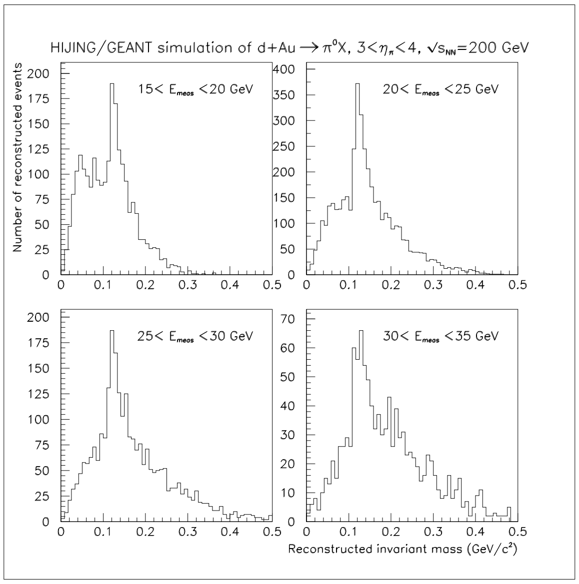

Figure 9: *Reconstructed invariant mass from HIJING/GEANT simulations of the response of a FPD calorimeter, including two orthogonal planes of a shower maximum detector, to d+Au collisions at* $\sqrt{s_{NN}} = 200GeV$. *The reconstructed* π^0*'s are at large rapidity (*$3 \leq \eta \leq 4$*) in the direction of the incident deuteron beam.*

If there is no preshower detector, then the resolution of the total energy measurement is compromised. Increasing the radiator thickness improves the efficiency of the SMD for observing the pair of daughter photons, but it does so at the expense of the calorimeter resolution. Simulations suggest that positioning a three radiation length converter (1.6 cm lead sheet) upstream of the Pb-glass preshower detector provides the best compromise between mass and energy resolution. This converter, when used together with the Pb-glass preshower detector, gives approximately the same photon conversion efficiency as used in the prototype endcap electromagnetic calorimeter (see Appendix). Rather than a single encased lead sheet, the converter should be built up from one radiation length sheets to allow possible changes to its thickness during operation.

3.4 d+Au collisions

Simulations of the response of the Forward π^0 Detector (FPD) calorimeter, including two orthogonal planes of shower maximum detector positioned after a $5X_0$ thick preshower/radiator, to d-Au collisions were examined. Complete HIJING events were generated, and were used in GEANT simulations of particle interactions in a FPD calorimeter. The same algorithm used to reconstruct event data obtained with the prototype FPD was applied to these simulations. The algorithm analyzes the calorimeter events by identifying candidate $\pi^0 \to \gamma\gamma$ events by their characteristic transverse shower profile measured by the SMD planes. The reconstructed invariant mass distribution as a function of total energy deposited in the calorimeter is shown in Fig. 9.

As for the response of the FPD calorimeter to pp collisions, a background is observed below the π^0 mass peak at low energies. The origin of this background is explained in the preceeding sections. The additional particle flux at large rapidities introduces additional background at large reconstructed invariant mass for d-Au collisions compared to what is experimentally observed in pp collisions. It is expected that this background can be substantially reduced by tuning the reconstruction algorithm. At present, the reconstruction does not utilize the segmentation available in the calorimeter to discriminate energy associated with the π^0 decay products from that deposited by other energetic ions intercepting the calorimeter. This additional information will be helpful to provide a cleaner signal from the FPD on the west side of STAR, corresponding to the direction of the deuteron beam, and hence the side that is sensitive to the gluon density in the gold nucleus. The additional information is absolutely critical for the FPD calorimeter mounted on the east side of STAR, corresponding to the direction of the Au beam.

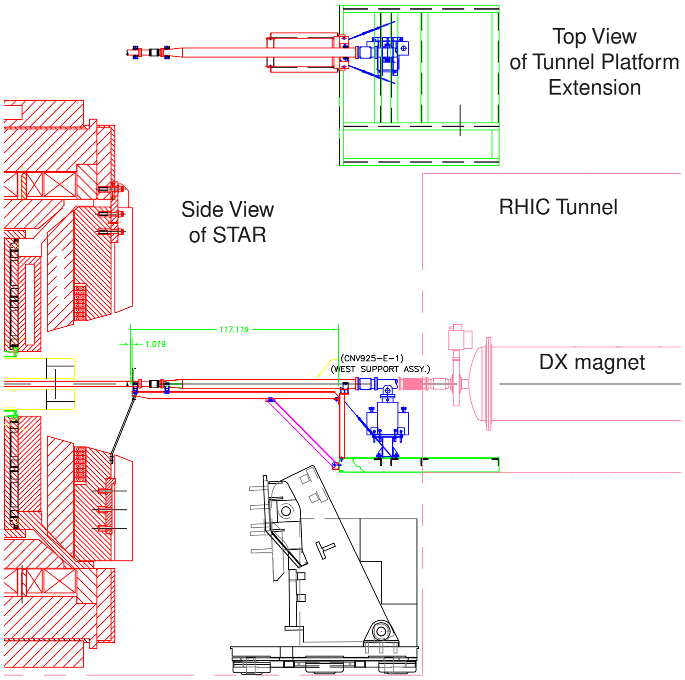

Figure 10: *A schematic of the STAR wide angle hall, showing the available space to the west of the STAR magnet. A platform extends into the wide angle hall at the same height as the tunnel to serve as the support for the beam pipe through the STAR magnet and for a pumping station. The east tunnel platform extension was used to mount electromagnetic calorimeters previously.*

4 Technical Description

The proposed Forward π^0 Detector involves mounting modular electromagnetic calorimeters to the left and right and above and below the beam on both the east and west tunnel platform extensions in the STAR wide angle hall. A schematic of the platform is shown in Fig. 10. Although there are tight space constraints, it was demonstrated with the prototype FPD last year that the two identical platforms in the STAR wide angle hall provide a good location for mounting forward calorimeters to enable the study of important physics topics involving identified particle detection at large rapidity.

The basic calorimeter module intended for mounting left and right of the beam is shown in Fig. 1. It consists of a light-tight box that contains a 7×7 matrix of existing Pb-glass detectors, FEU-84 photomultiplier tubes and resisitive voltage dividers. Each Pb-glass detector has dimensions of 3.7cm $\times$ 3.7cm $\times$ 45cm, and is wrapped in an aluminized mylar reflector. Two different types of Pb-glass are available. Approximately half of the Pb-glass detectors will be radiation hardened, resulting in a 10% loss of light output after a 10 krad dose. These detectors would be mounted close to the beam. The remaining detectors have 10% loss of light output after a 1 krad exposure. The Pb-glass detectors are coupled to a FEU-84 photomultiplier via a silicone disk. A resistive voltage divider, with a total resistance of 9.2 MΩ, provides the voltage differences to the twelve dynode stages of the FEU-84. The divider is typically operated at 1400 V and dissipates 0.2 W of power. The Pb-glass detectors, PMT's and voltage dividers are from an existing detector array built by the IHEP, Protvino group for E704 at Fermi National Accelerator Laboratory. Forty-eight of these detectors were successfully used as part of the prototype FPD during the FY2002 polarized proton run (see Appendix). Each PMT+base requires a high voltage cable to carry the 1400 V to each resistive divider, and a coaxial cable to carry the low power current pulses from the PMT anode to the readout electronics. Conventional SHV and BNC feedthroughs on the back plate of the box will be used for this purpose.

In addition to the primary electromagnetic calorimeter, the light-tight box would also house a pair of scintillator strip shower maximum detectors (SMD) needed to measure the diphoton opening angle with sufficient resolution. Two such SMD planes are required, with the strips mounted in orthogonal directions. The SMD planes are constructed from extruded plastic strips having a triangular cross section. The apex to base height of the triangle is 0.7 cm and the base length is 1.0 cm. The strips are wrapped in aluminized mylar reflectors, and then glued together to form a planar detector. The resulting SMD plane has a rectangular cross section tiled by alternating upward and downward pointing triangular strips. After the planes are glued, the resulting assembly can be machined to the requisite dimensions. To span the transverse dimensions of the 7×7 Pb-glass matrix, each SMD plane must have dimensions of 26 cm $\times$ 26 cm, and is constructed from 48 strips having a length of 26 cm. Scintillation light is collected by inserting 0.83 mm diameter, Y-11 doped wave-length shifting (WLS) optical fibers that are mirrored on one end into a co-extruded hole that runs the length of the scintillator strip. The light is transported to one of sixteen individual pixels of a Hamamatsu H6568 multi-anode photomultiplier tube (MAPMT) via the WLS fiber. Since the SMD and the MAPMT are contained within the same light-tight box, no additional optical connections are required; the WLS fiber serves a dual role of scintillation light collection and transport to the MAPMT. Each fiber must have a length of $\sim$60 cm to run along the full length of the scintillator strip, and to transport scintillation light to MAPMT that are mounted in the light-tight box. The fibers are glued into a square plastic holder with a 4×4 matrix of holes at a pitch that is matched to the pixel size of the MAPMT. After gluing, the fiber holder assembly must be polished to maximize the light transmission to the MAPMT. A frame presses the fiber holder to the rigidly mounted MAPMT within the light-tight box. Electrical feedthroughs carry the signals from the MAPMT to electronics described in the following section.

The interior of the light tight box would have plates to hold the 7×7 Pb-glass array in place, and also to rigidly mount and align the SMD planes. Extra volume inside the box is needed for routing optical fibers from the SMD strips to the MAPMT.

In front of the modular calorimeter, an array of 7 Pb-glass detectors would be mounted to serve as an active preshower detector. These detectors would be wrapped in black construction paper so as to be individually light tight. That same technique was used for the Pb-glass detectors of the prototype SMD mounted on the east platform extension for the first polarized proton run.

The calorimeter modules and preshower detectors would be elevated by 105 cm to beam height off of the tunnel platform extensions. The total weight of a fully loaded calorimeter box and its accompanying preshower detector is estimated to be $\sim$500 pounds, substantially less than the sampling calorimeter that was mounted on the east tunnel platform extension in 2001. An engineering design of suitable support stands that is compatible with the limited space available on the platform extensions is required.

For the calorimeters above and below the beam, we propose a simpler deployment, similar to what was installed for the prototype FPD. The basic calorimeter module would be a 5×5 matrix of Pb-glass detectors, limited by the space between the beam-pipe support stand. The individual Pb-glass detectors would be made light tight by wrapping them in black construction paper, as was done in the original design. The up and down calorimeters are extended compared to the original design to ensure adequate transverse size to fully contain the daughter photons from high energy π^0 decay.

5 Electronics and Trigger

The Pb-glass detectors, forming the basic elements of the calorimeter module and preshower detectors, are existing detectors, built by the IHEP, Protvino group for FNAL experiment E704. The outstanding physics opportunities at RHIC are the motivation to mount these detectors at STAR. The primary costs for this project are associated with the electronics to read out these existing detectors, and the manpower required to design, assemble and mount the calorimeter modules.

We propose to instrument individual photomultiplier tubes (PMT's) of the Pb-glass calorimeter with 8-bit analog-to-digital converters (CDB) that operate at the RHIC clock frequency. The interface to the STAR trigger and data acquisition system would be through Data Storage and Manipulation (DSM) boards that serve as a digital pipeline and field-progammable gate arrays that can be programmed to trigger on large pulse height events. Each DSM board services 16 channels of ADC. The total channel count of PMT's for the FPD calorimeter is 296, and corresponds to the channel count proposed for CDB's and DSM's.

We propose to encode the data from the scintillator strip shower maximum detectors (SMD) and the Pb-glass preshower detectors using an analog pipeline (switched capacitor array) and ADC system that has been developed for the preshower detector of the barrel electromagnetic calorimeter. A total of 412 channels of SCA/ADC are required for this purpose.

Each Pb-glass PMT and multi-anode PMT, used for the scintillator strip SMD, will be powered by a single channel of a multi-channel high voltage (HV) system, such as the LeCroy 1440. A total of 348 channels of HV are required for this purpose. Two separated HV systems are required, because the calorimeters are mounted on the east and west tunnel platform extensions, that are separated by $\sim$15 m.

The large number of HV and co-axial signal cables precludes mounting the electronics and HV systems on the south platform of STAR. All cables from the FPD and to the STAR electronics platform must be disconnected whenever the STAR magnet and mid-rapidity detectors move between the Wide-Angle Hall (WAH) and the Assembly Building (AB). To avoid the problem of continually connecting/disconnecting cabling, we propose to mount the high voltage and readout electronics systems on the east and west walls of the WAH. A Myrinet connection and a multi-conductor ribbon cable are required to interface the FPD electronics to the network and trigger electronics on the south platform of STAR.

6 Manpower, Installation Schedule and Project Cost

A team of interested physicists have personnel available at both their home institution and stationed at BNL to work on this project. Some of the groups on this proposal (*e.g.*, Texas A&M University) will be unable to contribute to the contruction of the FPD due to prior commitments to construction and installation of the STAR endcap electromagnetic calorimeter. They will, however, be active participants in the analysis of FPD data. The tasks involved in the project include:

- design/engineer light-tight boxes and support stands for the Pb-glass calorimeters and shower maximum detectors. This design must be compatible with the existing space on the tunnel platform extensions at STAR (Fig. 10. It is estimated that the design work and integration can be completed in four weeks.

- manufacturing of the calorimeter box walls and support stands required to mount the calorimeters at beam height. The total machining time is estimated to be four weeks. A more detailed estimate requires the completion of the design work.

- transport the Pb-glass detectors, presently at Jefferson Laboratory, to BNL. Members of the IHEP, Protvino team have already packed 280 detectors, including photomultipliers and resistive voltage dividers for transport to BNL.

- test/calibrate the individual Pb-glass detectors. It should be possible to utilize a $\sim$1 GeV secondary electron beam, available at the focal plane of the photon tagger spectrometer of the National Synchrotron Light Source at BNL for this purpose. A light-emitting diode system will be used to transfer this calibration for individually identified Pb-glass detectors from the test beam to their final location in the STAR wide angle hall. Final Pb-glass detector calibration will be performed *in situ* by reconstructing $\pi^0 \to \gamma\gamma$ decays as described in Sect. A.3. The effort involved in the test beam studies is estimated to require two physicists working for three weeks to calibrate each of the 324 Pb-glass detectors planned for the FPD.

- manufacture the scintillator strip shower maximum detector (SMD). The techniques for SMD assembly have been refined by the ANL group from their experience of building similar, but much larger scale detectors, for the STAR endcap electromagnetic calorimeter project. The process involves first wrapping the existing extruded scintillator strips with aluminized mylar reflectors, and then the alignment and gluing of alternating apex-up and apex-down strips to form planar detectors. This work will be performed at ANL by physicists and/or students affiliated with the participating institutions listed above. Based on the experience of the ANL group, it is estimated that 3 man-weeks of work at ANL is required to produced the requisite

Component	Channel Count	Cost
Calorimeter electronics: includes CDB,DSM, VME crates and cabling	296	$300,000
Shower maximum detector readout	412	$60,000
Multianode photomultiplier tubes, optical fibers	24	$40,000
Mechanical design, materials and machining		$80,000

Table 1: *Estimated costs for the STAR Forward π^0 Detector, consisting of a left/right symmetric pair of highly instrumented electromagnetic calorimeters positioned to both the east and west of the STAR magnet. Simpler calorimeters are placed above and below the beam at the two ends of STAR.*

SMD planes. Following assembly, an additional week of machining is needed to cut the SMD planes to the final dimensions.

- manufacture the optical fiber bundles that collect scintillation light from the scintillator strips, and transport it to pixels of a multi-anode photomultplier tube (MAPMT). We intend to have this work completed at Fermi Lab. Initial contact with the Particle Physics Division has been made, and final arrangements for the fiber preparation are being made.

- final assembly of the calorimeters will be done in lab space available in Building 510a at BNL. This work will involve assembly of the light-tight boxes, stacking of the Pb-glass detectors, installation of the MAPMT, and installation of the SMD planes with their fiber optic readout for each of the four calorimeter modules that are planned for symmetric placement to the left and right of the beam at both ends of STAR.

- installation of the assembled calorimeter modules on the tunnel platform extensions of the STAR wide angle hall.

- the CDB and DSM channels required for encoding the data from the FPD calorimeters, triggering and the interface to the STAR data acquisition system will be built at Lawrence Berkeley National Laboratory (LBNL). As well, the SCA/ADC system required for the encoding of data from the scintillator-strip shower maximum detectors and the Pb-glass preshower detectors will be built at LBNL.

The costs associated with the FPD project are listed in Table 1. Cost savings could be realized by summing current pulses from multiple PMT's prior to encoding the data. The prototype FPD tower granularity is approximately four times coarser than will be provided by the Pb-glass detectors, and is found to be sufficient from results obtained during the first polarized proton run at RHIC. Calorimeter granularity will reduce the background at large invariant mass for d-Au collisions and is essential for forward π^0's detected in the direction of the incident Au beam.

A time line for the completion of the FPD is shown in Fig. 11.

ID	Task Name	Duration	Start
1	**FPD**	**113d**	**Mon 7/1/02**
2	**electronics**	**93d**	**Mon 7/15/02**
3	DSM	70d	Mon 7/15/02
4	CDB	70d	Mon 7/15/02
5	SMD	80d	Thu 8/1/02
6	HV	60d	Thu 8/1/02
7	**Detector**	**60d**	**Mon 7/1/02**
8	PbGL	10d	Mon 7/1/02
9	PMTs	10d	Mon 7/15/02
10	Bases	5d	Mon 7/29/02
11	Calibration	20d	Mon 8/5/02
12	Fibers	60d	Mon 7/1/02
13	**Mechanical**	**45d**	**Mon 7/1/02**
14	design	10d	Mon 7/1/02
15	materials	20d	Mon 7/15/02
16	fab	10d	Mon 8/12/02
17	install	5d	Mon 8/26/02
18	installation	5d	Mon 9/23/02
19	Test	10d	Thu 11/21/02

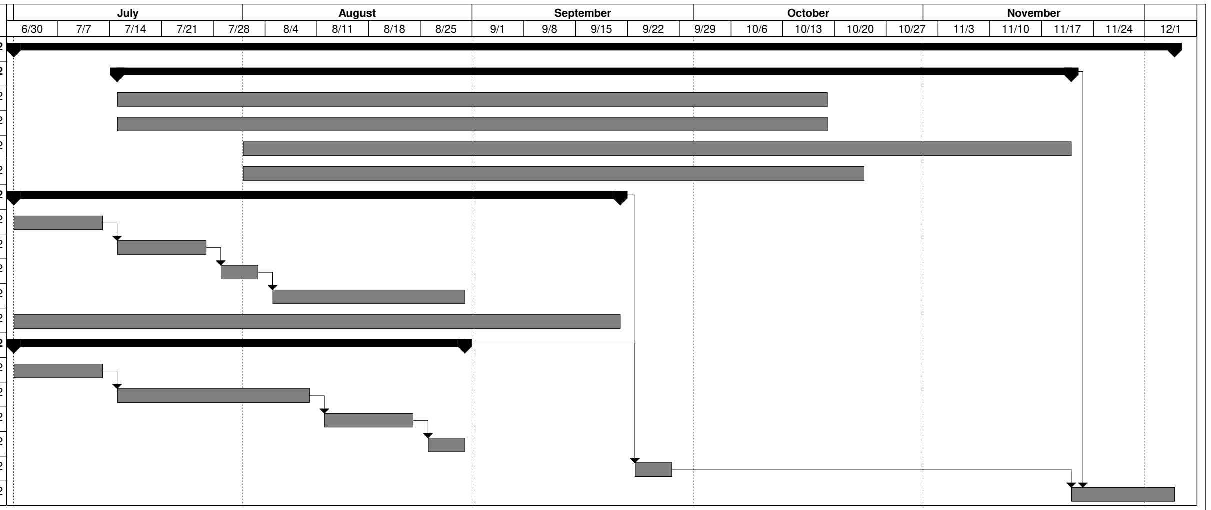

Project:
Date: Mon 6/3/02

Task | Milestone | Rolled Up Task | Rolled Up Progress
Progress | Summary | Rolled Up Milestone

Page 1

Figure 11: *A time line for completion of the FPD project*

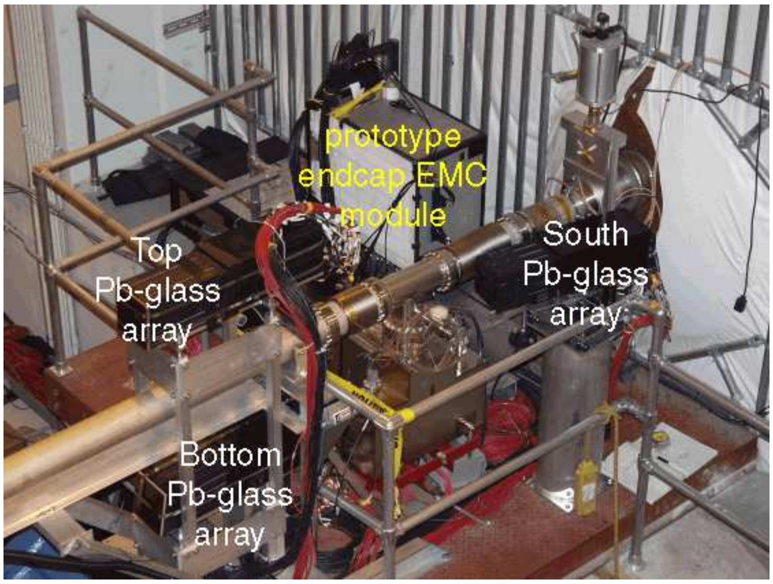

Figure 12: *Photograph of the east tunnel platform extension of the STAR wide angle hall showing the installation of the four calorimeters around the beam pipe. The north detector is a lead-scintillator sampling calorimeter, including preshower layers and a scintillator strip shower maximum detector. The other calorimeters are 4×4 arrays of Pb-glass detectors. The north and south detectors are displaced by 750 cm from the STAR interaction point.*

A Appendix: Results from prototype FPD measurements

A prototype Forward π^0 Detector (FPD) was mounted on the east tunnel platform extension in the STAR wide-angle hall during the first RHIC polarized proton run. A picture of the detector arrangement is shown in Fig. 12. The intent of this prototype was to establish the detector technology needed to cleanly reconstruct π^0 events in close proximity to the beam but distant from the STAR interaction point. This capability was intended to enable the study of spin observables at large Feynman x and moderate p_T. This prototype FPD was constructed from two different detector technologies listed below, but lacked the left/right symmetry required of a polarimeter. The prototype FPD was comprise of:

- a lead-scintillator sampling calorimeter. This detector is a prototype of the STAR endcap electromagnetic calorimeter (pEEMC), and included a shower maximum detector (SMD) having two orthogonal planes of scintillator strip detectors to measure transverse shower profiles. The first two sampling planes had individual tile readout to serve as a preshower detector. The preshower detectors and SMD provides information about the longitudinal development of the detected showers. Prior to installation at STAR, the pEEMC had been extensively studied

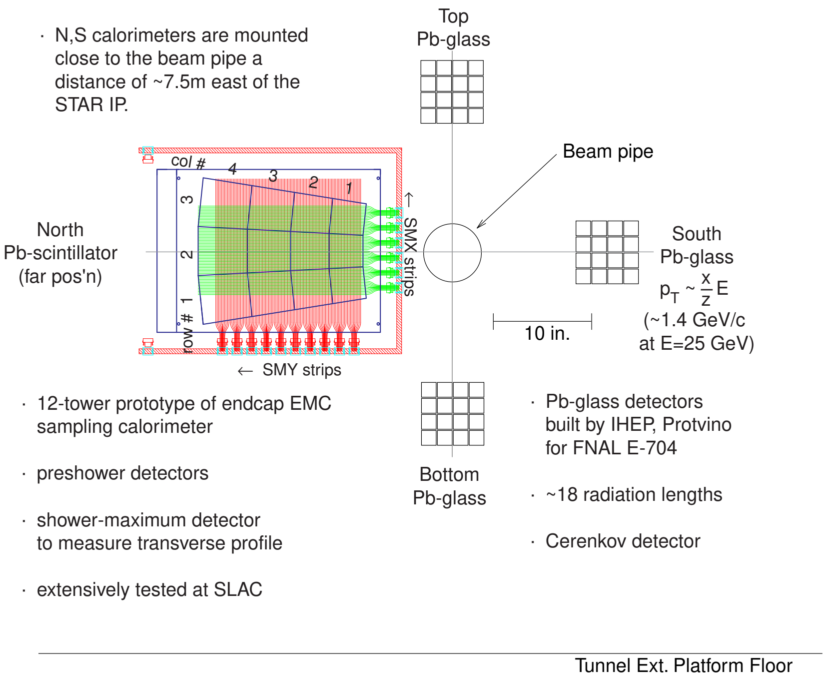

Figure 13: *Schematic of the prototype Forward π^0 Detector that was installed on the east tunnel platform extension of the STAR wide angle hall prior to the polarized proton run. The vantage in this schematic is from the east poletip of the STAR magnet, looking to the east. The calorimetery is displaced by 750 cm from the STAR interaction point along the beam line.*

with high energy electrons in a test beam at SLAC.

- three arrays of 3.8 cm $\times$ 3.8 cm $\times$ 45 cm lead-glass detectors. These detectors were built by the IHEP, Protvino group for experiment E-704 at Fermilab. Each array had sixteen Pb-glass detectors arranged in a 4$\times$4 matrix. The arrays were positioned above, below and to the south of the beam, in close proximity to the beam pipe.

A schematic of the FPD calorimetery that was installed in the STAR wide angle hall for the first polarized proton run is shown in Fig. 13. This section summarizes the performance of these detectors, and provides the justification for the choice of technology for a complete FPD for STAR in this proposal.

A.1 Event triggering for prototype FPD

Existing CAMAC electronics were used to encode data from the prototype FPD. Conventional gated ADC's, with long ($\sim 5\mu$s) conversion times were employed. These ADC's required a trigger decision on a time scale that was substantially faster than available from the STAR level-0 trigger. This trigger was derived from the calorimeter response. Read out of the FPD data was initiated when the summed current pulse from all PMT's of one of the four calorimeters exceeded a threshold. The

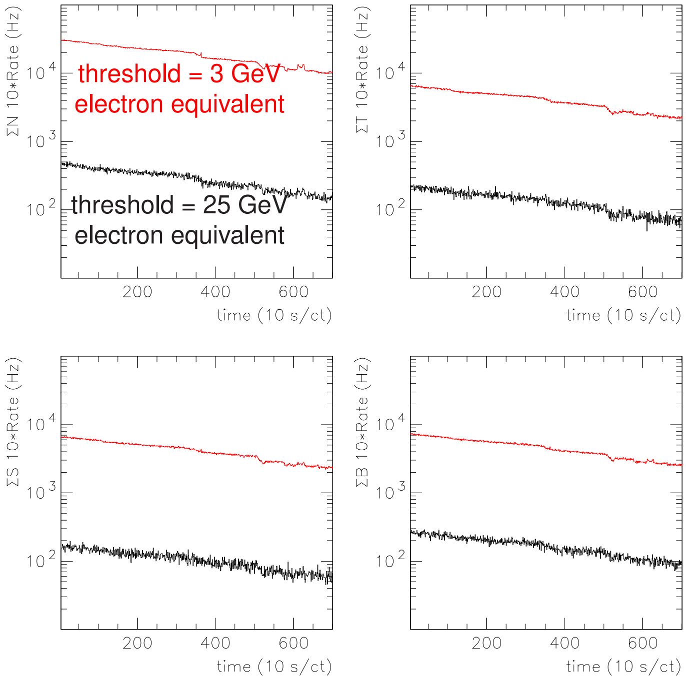

Figure 14: *Count rates from the FPD calorimeters above ∼20 GeV and ∼3 GeV electron-equivalent thresholds. The north calorimeter is in its 'near' position. This data is for a run recorded during RHIC fill 2175. The luminosity at the start of data recording was* $\sim 0.4\times10^{30}$ $cm^{-2}s^{-1}$*, as determined by the STAR beam-beam counter count rate. The count rate decreases approximately as an exponential function of time at a rate that is consistent with the beam lifetime.*

event trigger was an OR of the separately enabled threshold crossings from the north, south, top and bottom calorimeters. The current sums from the PMT's were added for each calorimeter either by rows or by columns, progressively distant from the beam. Separate discriminators were used to establish when each of these subsets crossed threshold, with the results input to scalers.

A.2 Rates measured with prototype FPD

Since the calorimeters were in close proximity to the beam, there is the potential for high rates in the detectors arising from particles either from the collision or from 'beam-gas' backgrounds. High counting rates can compromise the detector performance, either through pileup effects or through variations of the photomultiplier tube gains. A scaler system was used to measure singles rates in the calorimeter continuously during the polarized proton run. The PMT gains were monitored as described in Section A.3.

One indication of the contributions to the FPD trigger is given by examining the time dependence of the counting rates measured during a Van der Meer scan as shown in Fig. 15. In this procedure the beams are locally steered at the STAR interaction point, first horizontally and then vertically, to measure the transverse beam dimensions, thereby determining the luminosity. Typically at STAR,

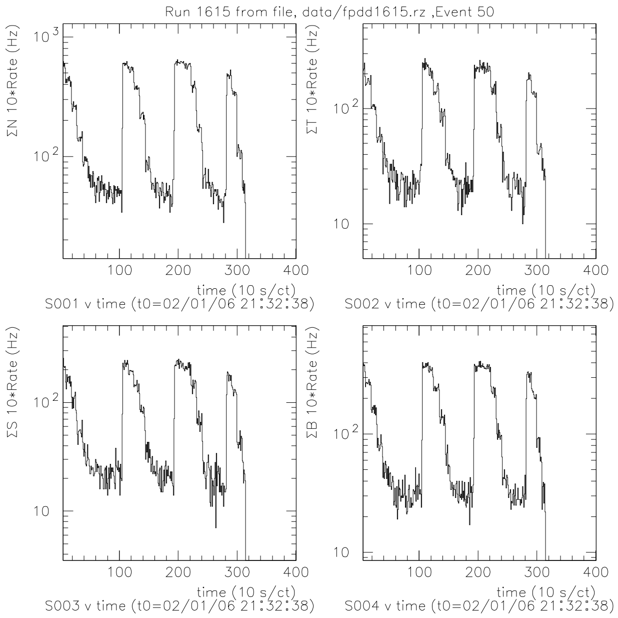

Figure 15: *Count rates from the FPD calorimeters above a ∼20 GeV electron-equivalent threshold. The north calorimeter is in its 'near' position. This data is for a run recorded during RHIC fill 2151. The luminosity for this fill is* $\sim 0.9 \times 10^{30}$ $cm^{-2}s^{-1}$. *A Van der Meer scan, corresponding to a systematic relative steering between the two beams at the STAR interaction point, was conducted during this run. The calorimeter count rates decrease by approximately a factor of 10 when the beams are out of collision, consistent with only a 10% contribution from 'beam-gas' events during this fill. The background rates depend strongly on the RHIC fill, and were continuously monitored by measuring the FPD count rate for bunch crossings corresponding to the Blue ring abort gap.*

the beam-beam counter coincidence rate was monitored during these scans to provide a signal of the extent that the beams were in collision. The relative contributions of backgrounds (so-called 'beam-gas' events) and *pp* collisions to the FPD high-threshold trigger rate can be determined from measurements made during the scan, by comparing the trigger rates when the beams are in collision *vs* when they are out of collision. For this particular fill of RHIC, 90% of the FPD triggers come from collisions. The signal:background ratio is found to be the same for all four calorimeters. The background fraction strongly varies for different fills as determined by monitoring the number of events for bunch crossings corresponding to the Blue ring abort gap (Fig. 16). From the STAR bunch crossing scalers, it is determined that the background of ≥20 GeV electron equivalent pulses from the north or south calorimeters is predominantly produced by beam gas events in the Yellow ring. To minimize the number of events from beam-gas backgrounds, only FPD events that have a coincidence with the east and west beam-beam counters are included in the data analysis briefly described below.

Overall, the counting rates in the calorimeters when the beams were in collision are shown in

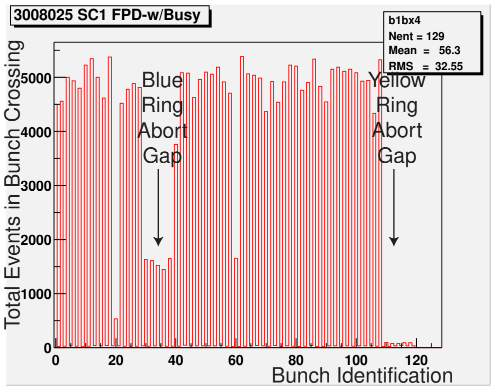

Figure 16: *Total counts from recorded by the STAR bunch-crossing scaler system for FPD events. An event is defined as either the north or south calorimeter crossing a ~20 GeV electron equivalent threshold, and includes a veto when the FPD data acquisition system (DAQ) was already busy. The live time is measured to be 85%. Note that the background from Blue ring beam gas events is much smaller than from the Yellow ring. At STAR, the beam in the Yellow ring is directed towards the east. The prototype FPD was mounted east of the STAR detector.*

Calorimeter towers	E≥20 GeV rate (kHz)	E≥3 GeV rate (kHz)
North	0.12	75
South	0.05	20
Top/Bottom (average)	0.05	18

Table 2: *Counting rates in FPD calorimeters normalized to a luminosity of 10^{30} cm^{-2} s^{-1} for pp collisions.*

Table 2. Based on the measured rates from the prototype FPD, we expect that for the proposed FPD configuration (Fig. 2), a single PMT from the calorimeter will have a rate of $\sim$ 10 Hz for $\geq$ 20 GeV energy deposited at a luminosity of 10^{31} cm^{-2} s^{-1}, and about two orders of magnitude larger rate for small ($\geq$ 3 GeV) energy deposition pulses. Based on measured rates and predicted analyzing powers, the overall count rate in a calorimeter module should provide sensitivity to vertical or radial beam polarization components of magnitude 0.1 within a single RHIC store. This is further discussed in Sect. 2.3.

A.3 Calibration of prototype FPD

To permit the event-by-event reconstruction of neutral pions, it is essential to have reliable gain calibrations of the photomultiplier tubes (PMT) used to collect scintillation light from individual strips of the shower maximum detector (SMD), and the PMT's that collect scintillation light from the sampling calorimeter towers or the Cerenkov radiation from the Pb-glass detectors.

For individual SMD strips, cosmic-ray muons have successfully been used to accurately determine the effective gain of individual scintillator strips. The procedure is to acquire a sample of normally

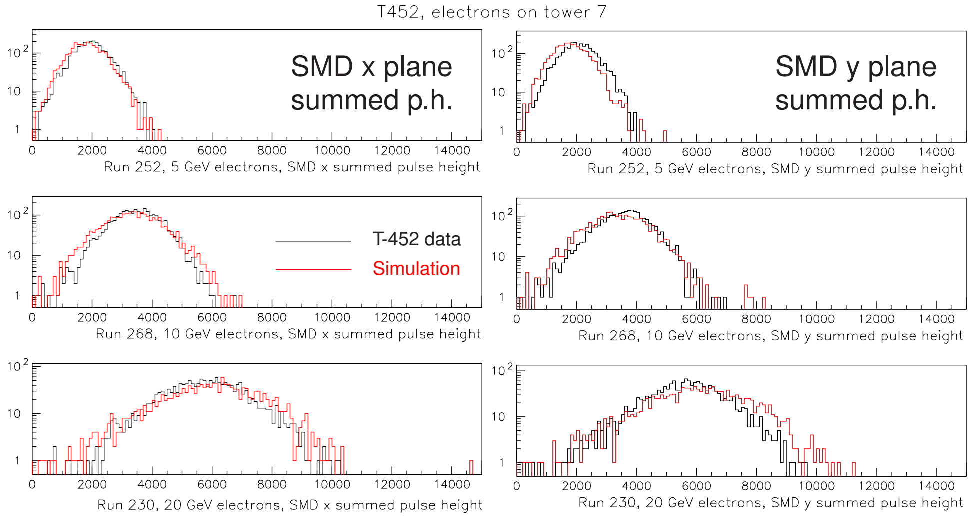

Figure 17: *Summed ADC distributions from scintillator strips that sample electromagnetic showers produced by single 5- (top), 10- (middle) and 20-GeV (bottom) electrons incident on the prototype endcap EMC module that were measured in test-beam experiment T-452 at SLAC. The gain matching of the response of indiviudal strips is done using cosmic ray muons following a procedure described in the text. The data are compared to simulations that account for the shower sampling and the PMT response. For the latter, it is assumed that a single photoelectron delivers* 3.8 ± 1.3 *pC of charge.*

incident cosmic ray muons. To identify events where the muons penetrate along the apex-to-base line of the triangular cross section strips, events are selected that have a current pulse from a single strip, but not from its neighbors. For these events, the mean value of the resulting integrated current distributions is determined for each strip. That value is associated with the inverse of the effective strip gain, corresponding to the product of the light collection efficiency of the optical fiber, the quantum efficiency of the pixel of the multi-anode photomultiplier tube (MAPMT), and the gain of the MAPMT dynode chain. This procedure had been employed as a calibration prior to in-beam tests of the prototype endcap electromagnetic calorimeter and its SMD planes at SLAC, using beams of 5, 10 and 20 GeV electrons. From the test beam data, the response from all strips to showers produced by the electrons is summed and compared to simulations that assume perfect gain matching. This comparison is shown in Fig. 17.

Several features should be noted from Fig. 17:

- The procedure of calibrating the strip response using minimum ionizing particles is a robust method of determining the individual effective gains of the scintillator strips.

- The SMD planes alone provide a crude determination of the incident electron energy, providing a resolution of $\delta E/E = 0.3/\sqrt{E}$. It will be shown in the following section that this resolution is sufficient to allow the reconstruction of neutral pions.

The tower response of the north calorimeter was also studied during the running of T-452 at

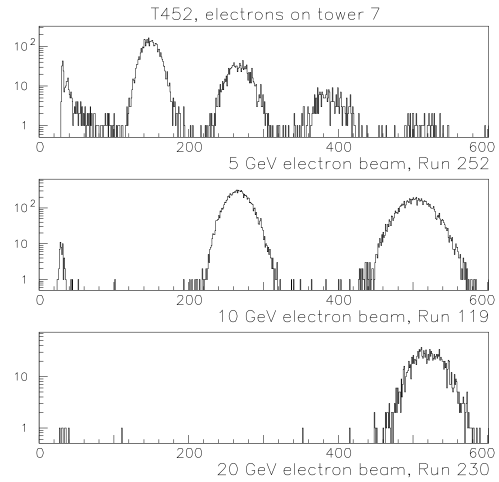

Figure 18: *ADC distributions observed during SLAC test beam experiment T-452 for the response of one of the north calorimeter towers to 'beams' of 5- (top), 10- (middle) and 20-GeV (bottom) electrons. The beam consists of a tunable number of high-energy electrons delivered within a 1 ps pulse at a repetition rate of 10 Hz. The peaks, with exponentially falling amplitude, at a single energy correspond to 1-, 2-, 3- and more electrons per pulse.*

SLAC. Six of the twelve calorimeter towers were scanned through the electron beams. The beams consist of a tunable number of high-energy electrons in a 1-ps bunch. Bending magnets selected secondary electrons produced at SLAC, and separate runs were taken with 5-, 10- and 20-GeV settings. Slits mounted upstream and downstream of the momentum analysis magnet define a beam with an absolute energy definition to 1% and a substantially smaller beam energy spread. The response of one of the towers of the north calorimeter to the electron test beams is shown in Fig. 18. Evident in the figure is the exponentially decreasing probability for events with one-, two-, three- or more high energy electrons. Small drifts of the ADC pedestals account for the small offsets of the peaks observed in these spectra. Events with a large number of high energy electrons enable the study of the linearity of the PMT response. The latter is found to be linear for current pulses corresponding to 160 GeV energy deposition.

The final determination of the calorimeter tower gains employed an *in situ* calibration. Events were classified by which calorimeter tower was found to have the largest energy deposition. The reconstructed invariant mass, discussed in the subsequent section, was then correlated with this 'high' tower. Software gain factors were adjusted to ensure that the centroid of the invariant mass peak for each 'high' tower was consistent with the mass of a neutral pion. There are sufficient statistics to separately determine the tower PMT gains for each RHIC store. Gain drifts are possible for different stores because the background counting rates are observed to vary.

A.4 π^0 Reconstruction

A scintillator strip shower maximum detector (SMD) is the key element to enable a robust identification of $\pi^0 \to \gamma\gamma$ for π^0's produced even to very high energies. The critical ingredients of the detection scheme are an accurate measurement of the opening angle between the two photons, an accurate determination of the *total* energy of the two photons, and only a coarse measurement of the *individual* photon energies. Separately, a tower-based calorimeter is used to measure the total energy of the neutral meson by containing the showers induced by the daughter photons. The SMD is then used to make the opening angle measurement and the crude determination of how the π^0 shares its energy between its daughter photons. The latter can be simply understood by viewing the SMD as a crude calorimeter. Test beam studies have demonstrated that the energy resolution of the SMD as a separate calorimeter is $\sim 30\%/\sqrt{E}$ (Fig. 17). This detector is also critical for the identification of single-photon showers.

The transverse shower profile, energy deposition in the towers and the preshower response for a single event are shown in Fig. 19. The two peaks in the energy deposition versus strip distribution for the orthogonal SMD planes are associated with the two photons from π^0 decay. The issue is to train software to be adept at identifying this event topology, so readily apparent when visually scanning events. Software to perform this task has been developed, although refinements are still in progress. The results of the event analysis are superimposed on the Fig. 19. In this event, an energy of 35 GeV was deposited in the calorimeter towers. From the tower response alone, there is insufficient resolution to observe the two photons from π^0 decay. That signature is clearly observed in the transverse shower profile, fitted by functions that quantitatively describe the SMD response. The centroids of each peak in the two orthogonal SMD planes accurately determine the di-photon separation to be 5.3 cm. The area under the peaks is used to crudely measure how to divide the summed calorimeter tower response amongst the individual photons. For this event, the two planes agree on this ratio to within 2%. The combined information from the SMD and calorimeter towers is consistent with interpreting the events as a $\pi^0 \to \gamma\gamma$ decay. The methodologies employed for event reconstruction are readily adapted to the endcap EMC because of the strong similarities between the hardware devices. The end result for events collected during the $\vec{p} - \vec{p}$ run is the invariant mass spectrum shown in Fig. 20.

As discussed in Sect. 3, the background observed in the measured invariant mass distribution is also present in simulations of the detector response. This background is found to decrease at higher energies, as shown in Fig. 8. The invariant mass resolution is roughly constant over the entire energy range, whose upper end is limited by statistics. It is expected that the invariant mass resolution will persist for π^0 energies of approximately 100 GeV, corresponding to a minimum diphoton opening angle of 2.7 mrad and a spatial separation of the photon clusters at the SMD of 2 cm. For higher energies, the overlap of the transverse profiles will not permit a robust separation at the SMD.

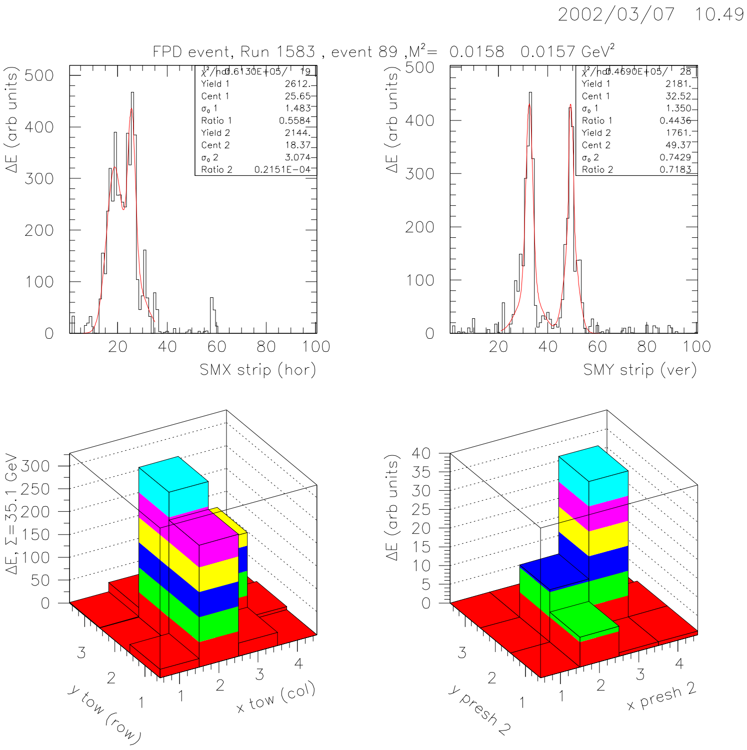

Figure 19: *Response of the scintillator strip shower maximum detector planes, calorimeter towers and preshower detector to a high-energy event in the prototype endcap EMC module. The upper row of figures shows the transverse shower profile measured in two orthogonal planes. Electromagnetic showers from a pair of high energy photons are evident in this event. The tower response (lower left) does not have sufficient granularity to identify the event as a pair of photons. The measured energy deposition versus strip number is represented by a function that describes the transverse profile of electromagnetic showers. The difference in centroid between the two orthogonal planes accurately measures the di-photon opening angle. The summed energy deposition in the SMD is used to determine how the* π^0 *energy is shared between its daughter photons.*

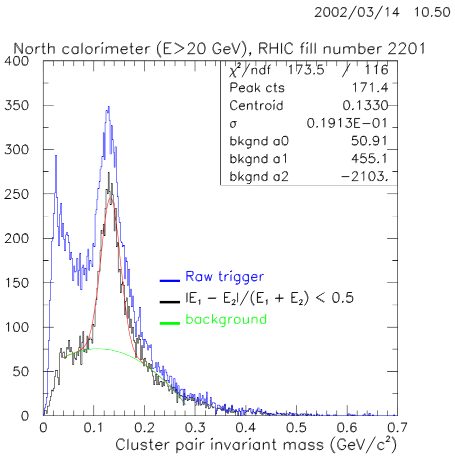

Figure 20: *Reconstructed invariant mass of events with identified cluster pairs. The energy threshold is 15 GeV (electron equivalent), and as shown in Fig. 8, the particle identification is robust up to the highest energies where events are observed. It is expected that above ∼100 GeV, the opening angle cannot be observed even with a SMD.*

This upper energy should be sufficient to identify π^0's out to at least x_F of 0.25 when RHIC is operated at a *pp* collision energy of $\sqrt{s} = 500$ GeV, enabling a program of A_N measurements and providing the possibility of an *in situ* polarimeter over the full range of RHIC energies. The shower maximum technology is better suited to such measurements than simply increasing the granularity of a conventional tower calorimeter.

Although data analysis continues, many correlations of the reconstructed invariant with other measured quantities have been studied and compared to expectations from simulations. One such correlation is between the reconstructed invariant mass and the photon energy sharing, measured by the shower maximum detector. For the decay of the pseudoscaler pion, the photon energy sharing distribution must be uniform. By two-body decay kinematics, the energy sharing is correlated with the diphoton opening angle. Large energy asymmetries correspond to back-to-back photons, which cannot be observed with the FPD calorimeters, and equal energy photons (zero energy asymmetry) are decays at the minimum opening angle between the two photons. As expected, the photon energy sharing in the vicinity of the neutral pion mass is observed to be uniform until one photon is three times more energetic than the other. Decays with greater asymmetry are not observed because the diphoton opening angle is too large compared to the calorimeter acceptance. The background in the invariant mass distribution arises primarily from the misidentification of a single photon as a photon pair by one or both shower maximum detector planes. Such misidentifications occur when there are fluctuations in the transverse profile of an electromagnetic shower in the calorimeter resulting in a small satellite peak in the SMD response. These small secondary peaks mimic the signature expected from the $\pi^0 \to \gamma\gamma$ decay. These fluctuations, in general, arise from only a small fraction of the total shower energy, and are reconstructed as events with small opening angles and large energy

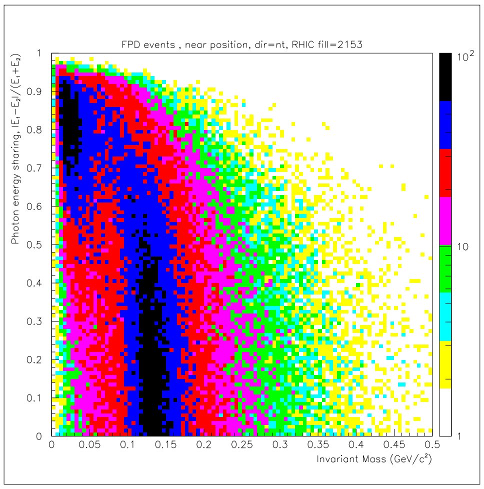

Figure 21: *Correlation between the reconstructed invariant mass and the photon energy asymmetry for data obtained with the north calorimeter of the prototype FPD. As shown in Sect. 3.1, pion decay results in a uniform photon energy asymmetry distribution. The largest energy asymmetries correspond to large diphoton opening angles, beyond the acceptance of the detector. Backgrounds in the invariant mass distribution arise when the SMD misidentifies single photon events as a pair of clusters because of fluctuations in the transverse profile of electromagnetic showers in the calorimeter.*

asymmetries.

References

[1] L. McLerran, *The color glass condensate and small x physics: 4 lectures*, Lectures given at 40th Internationale Universitatswochen fuer Theoretishche Physik: Dense Matter (IUKT 40), Scladming, Asutria, 3-10 Mar 2001, hep-ph/0104285.

[2] A.H. Mueller, *Small-x Physics, High Parton Densities and Parton Saturation in QCD*, hep-ph/9911289. Published in *Lisbon 1999, QCD: Perturbative or nonperturbative?*, pp. 180-209.

[3] Adrian Dumitru and Jamal Jalilian-Marian, BNL Report no. BNL-NT-02/7 and hep-ph/0204028 (2002).

[4] M. Arneodo, Phys. Rep. **240** (1994) 301.

[5] NMC collaboration, M. Arneodo *et al.*, Nucl. Phys. **B481** (1996) 23.

[6] K.J. Eskola, V.J. Kolhinen and P.V. Ruuskanen, Nucl.Phys. **B535** (1998) 351.

[7] HERMES collaboration, A. Airapetian *et al.*, Phys. Rev. Lett. **84** (2000) 4047.

[8] M. Anselmino and F. Murgia, Phys. Lett. B 483 (2000) 74.

[9] H.O. Meyer, Phys. Rev. C **56** (1997) 2074.

[10] W. Vogelsang, *Theory Topics in Year-1 and Beyond*, talk given at RHIC Spin Collaboration Meeting VI, 1 October 2001, BNL report 52642.

[11] T. Sjöstrand, Comp. Phys. COmmun. **82** (1994) 74.

[12] J. Soffer, Phys. Rev. Lett. **74** (1995) 1291; D. Sivers, Phys. Rev. **D51** (1995) 4880.

[13] H.M. Spinka *et al.*, *Proposal to Install a Forward π^0 Detector in STAR*, (2001) available at http://www.iucf.indiana.edu/~bland/polar_proposal.ps.gz

[14] D. L. Adams, *et al.*, Phys. Lett. B**261**(1991)201.

[15] D. L. Adams, *et al.*, Phys. Lett. B**264**(1991)462.

[16] D. W. Sivers, Phys. Rev. D **41**, 83 (1990) [Annals Phys. **198**, 371 (1990)].

[17] M. Anselmino, M. Boglione and F. Murgia, Phys. Rev. D **60**, 054027 (1999) [arXiv:hep-ph/9901442].

[18] M. Anselmino, A. Drago and F. Murgia, arXiv:hep-ph/9703303.

[19] Vincenzo Barone, Alessandro Drago, Philip G. Ratcliffe, Phys. Rept. **359** (2002).

[20] S. J. Brodsky, D. S. Hwang and I. Schmidt, Phys. Lett. B **530**, 99 (2002) [arXiv:hep-ph/0201296].

[21] J. Qiu and G. Sterman, Phys. Rev. D**59**(1998)014004.

[22] F.S. Bieser, H.J. Crawford, J. Engelage, G. Eppley, L.C. Greiner, E.G. Judd, S.R. Klein, F. Meissner, R. Minor, Z. Milosevich, G. Mutchler, J.M. Nelson, J. Schambach, A.S. VanderMolen, H. Ward and P. Yepes, to be published in Nucl. Instr. and Meth. (2002).